

# Empirical Descriptors Evaluation for Mass Malignity Recognition

Imene Cheikhrouhou<sup>1,2</sup>, Khalifa Djemal<sup>1</sup>, Dorra Sellami Masmoudi<sup>2</sup>  
Hichem Maaref<sup>1</sup> and Nabil Derbel<sup>2</sup>

<sup>1</sup> University of Evry Val d'Essonne (UEVE), France

<sup>2</sup> National Engineering school of Sfax (ENIS), BP W, 3038 Sfax, Tunisia

**Abstract.** In breast cancer field, radiologists and researchers aim to discriminate between masses due to benign breast diseases and tumors due to breast cancer. In general, benign masses have circumscribed contours, whereas, malignant tumors appear with spiculated and irregular boundaries. Recently, we proposed an original mass description based on three morphological mass descriptors, which are SPICULATION (SPICUL), Contour Derivative Variation (CDV) and Skeleton End Points (SEP). In this paper, we detail an empirical mass evaluation based on these morphological descriptors which intend to distinguish between malignant and benign lesions. This evaluation is, first, assured by following descriptors evolution in two independent data sets: Alberta and MIAS. Secondly, for these two data sets, the Receiver Operating Characteristics (ROC) analysis is applied. A comparison between the classic use of Area (A) and Perimeter (P) descriptors only, and a combination with our three original evaluated descriptors is done. Obtained results proves that classification accuracy of the descriptors combination including: SPICUL, SEP, CDV, A and P outperforms that of the classic descriptors: A and P. Indeed, our original mass description provides the best Area under ROC  $A_z = 0.986$  for Alberta data set and  $A_z = 0.9792$  for the MIAS data set. Therefore, we affirm that our three original descriptors can serve as good shape descriptors for the benign-versus-malignant classification of breast masses on mammograms.

## 1 Introduction

Breast cancer is one of the most common diseases that threaten woman life and scientific studies have shown that the mortality rate caused by breast cancer is decreased by early detection and treatment. Mammography is known to be the most effective screening method and is credited with reducing breast cancer mortality by at least 30%. However, screening mammography program requires a large number of radiologists with special training in this field which could involve problems such as high costs and visual fatigue. For this reason, several researches aim to develop Computer Aided Diagnosis systems (CAD) that could automatically analyze mammographic images [1], [2], [3]. These CAD systems focus on detection, description and classification of breast abnormalities which could be either a mass or a microcalcification, or sometimes both

[4] [5]. Breast Imaging Reporting and Data System (BIRADS) standard is a mammographic lexicon developed by American College of Radiology (ACR) [6] for the mammographic lesions description. This lexicon includes descriptors such as the mass margins and the microcalcification distribution that defines final assessment categories and suspicion level of mammographic abnormalities.

According to BIRADS, masses classification depends on contour complexity. The descriptors used to define masses are shape and margin [6]. A benign mass is a regular form, generally round or oval with a well circumscribed boundary, whereas a typical malignant tumor is an irregular, spiculated form with a rough boundary. There could be also, some unusual cases which cause difficulties in pattern classification studies [17]. Many works focus on mass classification with contour descriptors. A study by Chen, et al [1] reported 0.982 as the best area under the receiver operating characteristic (ROC) curve ( $A_z$ ) when using five new morphological features that concretize variations in boundary delineation. Guo et al [20] computed the fractal dimension to characterize the complexity of breast mass contour. Rangayyan and Nguyen [19] presented a study of fractal dimension including the ruler method and the box counting method that leads to  $A_z = 0.89$  and a study of fractional concavity that provides  $A_z = 0.88$ . Their combination yielded the highest area under the ROC curve of 0.93. Some studies focus on the evaluation of existing descriptors because of its significant importance in downstream treatments and final decision. This evaluation is in order to preserve pertinent descriptors and to propose improvements for the others. We have proposed microcalcification evaluation that brings to improve the rectangularity formulation [15] and hence, the classification accuracy.

We have proposed previously [14] three pertinent descriptors which could describe mass forms and that could be very useful in CAD systems. So, to prove their performance, mammographic images are first preprocessed to obtain filtered [21] and segmented [22] [16][13][18] masses to could focus on detailing a descriptor evaluation for mass malignancy recognition by means of two data sets Alberta and MIAS which represent variety of cases. Our main objective in this evaluation is to prove how descriptors react towards complexity contour. The paper is organized in four sections. Next section is preserved to the evaluation of the morphological descriptors: SPICUL, CDV and SEP applied to two different data sets Alberta and MIAS. Section 3 shows experimental results. ROC curves associated to both data sets are represented to validate features ability to discriminate between benign masses and malignant tumors. We present also, a comparison with other methods that characterize shape complexity in the same data sets. Finally, we conclude in section 4.

## 2 Descriptors Evaluation through Two Mammographic Data Sets

Evaluated morphological descriptors are Contour Derivative Variation (CDV), Spiculation (SPICUL) and Skeleton End Points (SEP) [14]. Selected descriptors for validation are evaluated through two data sets. The first data set B1 was obtained from Screen Test: the Alberta Program for the Early Detection of Breast Cancer [7] [8]. From this data set, we exploit 35 benign masses, most of which are circumscribed, and 35 malignant tumors, most of which are spiculated, as typically encountered in mammographic

images. The second data set named B2 is from the Mammographic Image Analysis Society (MIAS) database [9]. From which we use 28 benign masses and 28 malignant ones including circumscribed and spiculated cases in both benign and malignant categories. Spiculated benign masses and circumscribed malignant tumors are unusual, and tend to cause difficulties in pattern classification studies.

## 2.1 Contour Derivative Variation (CDV)

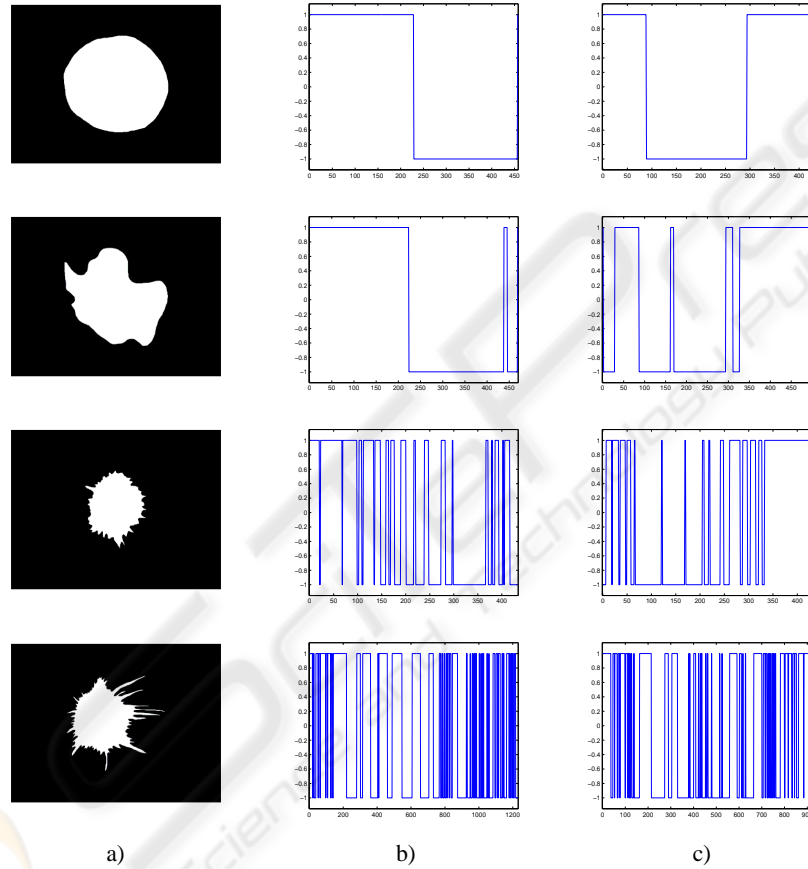


**Fig. 1.** Contour Derivative Variation related to X and Y: a) Original images, b) CDVX and c) CDVY.

As given in [14], for the  $k^{th}$  contour point with coordinates  $X(k)$  and  $Y(k)$ , we define the Contour Derivative related to x-coordinate (CDX) and Contour Derivative related to y-coordinate (CDY) as follows:

$$CDX(k) = \frac{X(k+1) - X(k-1)}{2} \quad CDY(k) = \frac{Y(k+1) - Y(k-1)}{2} \quad (1)$$

where  $X(k+1)$  and  $Y(k+1)$  are the  $(k+1)^{th}$  contour point coordinates, respectively,  $X(k-1)$  and  $Y(k-1)$  are the  $(k-1)^{th}$  contour point coordinates.

We note CDVX (resp. CDVY) the number of CDX (resp. CDY) variation sign from positive to negative or from negative to positive values. So, Contour Derivative Variation (CDV) is the CDVX and CDVY total sum.

Figure 1 shows images from the two data sets B1 and B2 ordered from benign to malignant. Subjectively, we can note that for regular masses we should have  $CDVX=2$  and  $CDVY=2$  as shown in fig.1, in the first image with circular shape which provides  $CDV=4$ . The second which is lobulated has low CDV value ( $CDV=12$ ). The last two images which are irregular and spiculated, have more sign variations in contour derivative. Especially for high spiculated masses as the forth<sup>th</sup> example, CDVX reaches 92 and CDVY reaches 88 which provides a high CDV value ( $CDV=180$ ). We can notice that CDV will increase considerably when contour becomes more and more complex.

To objectively prove this observation, we plot CDV values for both data set B1 and data set B2. Figure.2 a) shows all data set B1 images: from image  $n^o1$  to  $n^o35$ , we present benign images and from image  $n^o36$  to  $n^o70$ , we present malignant ones. Also, figure.2 b) shows all data set B2 images: from image  $n^o1$  to  $n^o28$ , we present benign images and from image  $n^o29$  to  $n^o56$ , we present malignant ones. We will preserve this distribution for all next evaluations. For data set B1, benign masses still under the value  $CDV=30$  and malignant ones are higher than  $CDV=30$  except of 7 images. For the second data set B2, benign images are all under  $CDV=30$  and for malignant cases, all images exceed this value except image  $n^o47$  with  $CDV=18$ . These results prove that this descriptor has the ability to distinguish between benign and malignant masses for the two data sets B1 and B2.

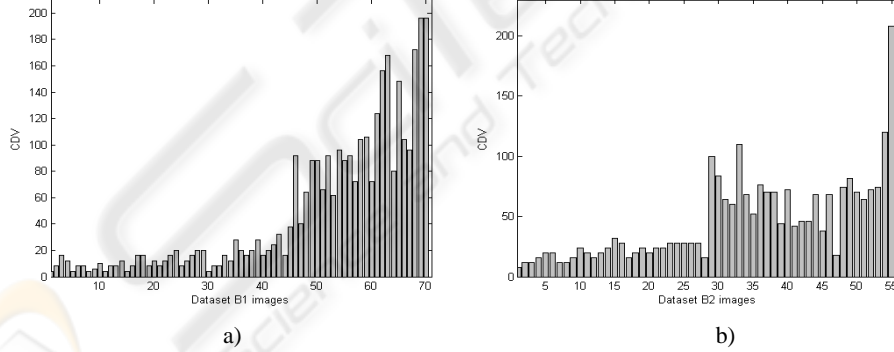


**Fig. 2.** CDV evaluation for: a) data set B1 and b) data set B2.

## 2.2 Spiculation (SPICUL)

In [14], we propose a new feature named spiculation (SPICUL) defined as follows:

$$S = \sum_k SpiculX(k) + \sum_k SpiculY(k) \quad (2)$$

where  $k$  represents the  $k^{th}$  contour point,  $SpiculX(k)$  (respectively  $SpiculY(k)$ ) is the number of points having the same x-coordinate (resp. the same y-coordinate). Masses from the two data sets, represented in fig.1 are reproduced in the same order of increasing malignity to be evaluated with the SPICUL descriptor. Results are given in Table 1 which shows that when the mass is more spiculated, (SPICUL) increases successively from 0.3967 to 6.0081.

**Table 1.** SPICUL value for six masses ordered from benign to malignant.

Mass 1	Mass 2	Mass 3	Mass 4
SPICUL 0.3967	0.6130	1.2514	6.0081

For evaluating the whole images, we show in fig.3 evaluation of the descriptor SPICUL. Data set B1 represented in fig.3 a) indicates that the first 35 benign images have nearly similar values which are all strictly under SPICUL=1. Otherwise, all benign masses are identified correctly. For malignant images, the majority of masses are well recognized and are well separated from benign masses with values between 2 and 6. But, 14 malignant cases are considered benign also. Data set B2 in fig.3 b) shows that SPICUL makes many errors in benign case recognition. So, SPICUL evaluation in data set B1 proves its strength to discriminate between malignant and benign images. And SPICUL evaluation, in data set B2, proves that errors are caused essentially by the presence of irregular forms in benign class that have higher SPICUL values.

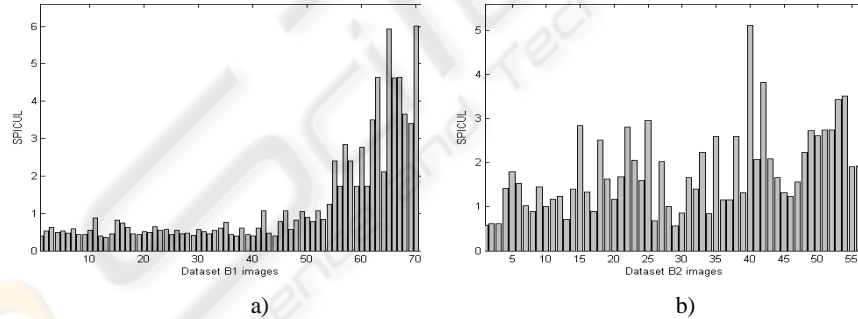


**Fig. 3.** SPICUL evaluation for: a) data set B1 and b) data set B2.

### 2.3 Skeleton End Points (SEP)

Skeleton provides a simplified version of the object at one pixel width. This representation makes easy complex images processing such as digital fingerprint, handwritten letters and [10] blood vessels images. In mammographic field, and especially when we treat complexity contour, skeleton seems to be very useful. In fact, for regular shapes, skeleton has few branches, and for irregular contours, skeleton becomes more complex

and has several ramifications. In [1] authors study skeleton concept in breast sonogram images by computing the number of skeleton points. This entity is very sensitive to lesion size. To avoid this constraint, we developed in [14] a new skeleton formulation adapted to our objectives, based on skeleton branches number by computing the number of skeleton End Points (SEP).

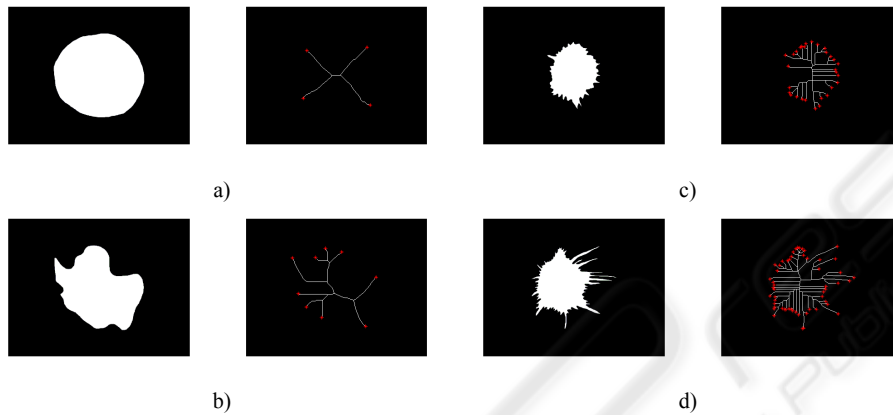


**Fig. 4.** Skeletonization: Four masses and relative skeletons with their end points (SEP).

As a first SEP evaluation, we plot in fig.4 skeletons and skeleton end points for the same masses studied in fig.1 and Table 1 extracted from B1 and B2. Fig.4 a) which is a regular circle have SEP=4. For the lobulated form b) SEP raises slightly with successively 7 ramifications. Irregular forms, (such as c and d) have skeletons more complicated and also have the higher SEP values such as the last mass d) with SEP=55. This first observation confirms the descriptor performance in distinguishing between regular and irregular masses, then between benign and malignant cases.

As a second SEP evaluation, we test SEP evolution across the two data sets in fig.5. We notice that, for fig.5 a), for the data set B1, benign masses could be visually distinguished with their low values under 13. However, for malignant masses, SEP highly increases with values that overpass SEP=50. The gap between SEP values favors discrimination between the two classes. For the data set B2, fig.5 b), benign forms are all recognized correctly ( all SEP values are  $\leq 13$ ). But, in malignant forms, the skeleton have some errors. It confounds some benign and malignant cases.

It should be noted that, for all evaluation examples, data set B1 recognizes better benign and malignant classes. And as we have said before, data set MIAS have some spiculated forms in benign class and some circumscribed forms in malignant class which clarify why this data set has less discrimination between the two classes. For this reason, we notice that descriptors for data set B2 translate well their information about complexity contour which explain that we find low descriptor values in malignant cases and high descriptor values in benign cases.

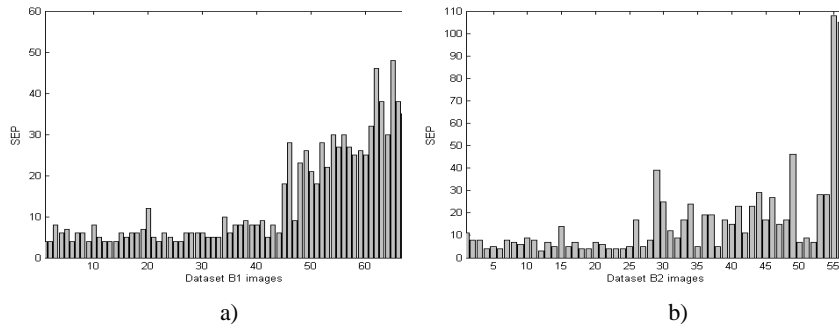


**Fig. 5.** SEP evaluation for: a) data set B1 and b) data set B2.

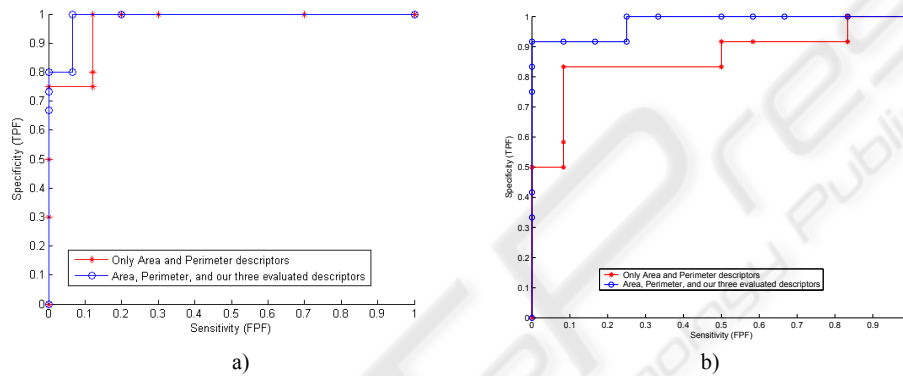


**Fig. 6.** ROC curve associated to: a) data set B1 and b) data set B2.

### 3 Experimental Results

Since mass classification depends on mass size, we compute mass area ( $A$ ) which is, in digital images, given by the number of pixels that belong to the mass. As a second geometrical feature, we add perimeter which can be easily obtained by computing boundary pixels [11]. These geometrical descriptors generally ameliorate classification rate. First, in this section, we use evaluated descriptors: CDV, SPICUL and SEP for classification through SVM classifier, joined to informative descriptors Area ( $A$ ) and Perimeter ( $P$ ). To evaluate the classification performance, we use the so-called Receiver Operating Characteristic (ROC) analysis, which is now used routinely for many classification tasks. A ROC curve is a plot of the classification sensitivity (TPF) as the ordinate versus the specificity (FPF) as the abscissa. For a given classifier, ROC curve is obtained by continuously varying the threshold associated with its decision function. At any given FPF, a ROC curve with a higher TPF corresponds to a better classification performance. The overall classification accuracy is summarized by the area under the ROC curve ( $A_z$ ).

In this section, we classify data set B1 and B2, first with all cited descriptors: Contour Derivative Variation (CDV), Spiculation (SPICUL), Skeleton end points (SEP),

Perimeter (P) and Area (A) (5 descriptors), and secondly with only P and A (2 descriptors) in order to keep a comparison between our proposed descriptors and known ones. These descriptors are used as entries to SVM classifier which seems to be an excellent candidate for several classification tasks such as medical applications [12].

Fig.6 a) shows ROC curve of data set B1 in both cases 5 descriptors and 2 descriptors. We notice that, although ROC curve of (5 descriptors) outperforms that of (2 descriptors), for both cases, TPF fraction still very high for FPF values. This proves the pertinence of descriptors adopted even for malignant images with similar aspect to benign ones and contrarily. Area under ROC computed for 5 descriptors is  $A_z = 0.986$  and for 2 descriptors is  $A_z = 0.97$  as given in Table 2.

Fig.6 b) represents ROC curve of data set B2 in both cases 5 descriptors and 2 descriptors. This data set contains circumscribed and spiculated masses in both malignant and benign cases. Although this new organization makes classification task very difficult, the area under ROC preserves a high value of  $A_z = 0.9792$  especially in the case of 5 descriptors. For two descriptors, classification accuracy decreases significantly and provides  $A_z = 0.854$  as shows in Table 2.

**Table 2.** Area under ROC for the two data sets.

$A_z$	Area and Perimeter	Area, Perimeter, SPICUL, CDV, and SEP
B1	0.97	0.986
B2	0.854	0.9792

We provide a final evaluation based on a comparison with a recent work. Rangayyan and Nguyen [19] focused on contour description on mammograms and detailed four methods to compute the fractal dimension of the contours of breast masses, including the ruler method and the box counting method applied to 1D and 2D representations of the contours. The methods were applied to the same data sets that we exploit: the Alberta [7] and MIAS [9] data sets. Receiver operating characteristics (ROC) analysis was performed to assess and compare the performance of fractal dimension methods and the use of the five descriptors: SPICUL, SEP, CDV, P and A in the classification of breast masses as benign or malignant. This comparison is presented in Table 3.

**Table 3.** Area under ROC for the two data sets in the case of fractal dimension and our descriptors.

$A_z$	Data set B1	Data Set B2
1D ruler	0.91	0.8
2D ruler	0.94	0.81
1D box counting	0.89	0.8
2D box counting	0.9	0.75
our descriptors	0.986	0.9792

We notice that, for the use of fractal dimension or our descriptors, data set B1 provides usually better results in classification than data set B2 because of the existence

of atypical masses (slightly lobulated or spiculated benign masses and round or circumscribed malignant tumors) which cause more misclassified cases than the data set B1. Also, the combination of the five descriptors: SPICUL, SEP, CDV, P and A outperforms the use of fractal dimension, that provides as better results with the use of 1D ruler method  $A_z = 0.94$  for data set B1 versus  $A_z = 0.986$  in our case and  $A_z = 0.81$  for data set B2 versus  $A_z = 0.9792$ .

## 4 Conclusions

In this paper, we propose an empirical evaluation of three morphological descriptors which are useful in the analysis of breast masses contours. For evaluation, we use two independent data sets from Alberta and MIAS. These data sets are widely different and independent which allows us to generalize from final results. When computing descriptors, we notice their ability to capture diagnostically important details of shape related to spicules and lobulations. The proposed descriptors, joined to the geometrical features perimeter and area, have provided high classification accuracies when discriminating between benign breast masses and malignant tumors. This result outperforms classification accuracy of the two descriptors P and A for the two data sets, which prove the performance and the precision of these descriptors. In future works, we intend to evaluate the performance of each descriptor apart and to compare them to other pertinent descriptors cited in literature which have proven a high performance in mass classification. Also, we intend to modify classification tools in order to reduce False Positive Fraction and to further maximize True Positive fraction.

## References

1. C-M Chen, Y-H Chou, K-C Han, G-S Hung, C-M Tiu, H-J Chiou, S-Y Chiou, "Breast Lesions on Sonograms: Computer-aided Diagnosis with Nearly Setting-Independent Features and Artificial Neural Networks", *Radiology*, Fvriar 2003, p504-514.
2. H-K Chiang, C-M Tiu, G-S Hung, S-C Wu, T-Y Chang, Y-H Chou, "Stepwise Logistic Regression Analysis of Tumor Contour Features for Breast Ultrasound Diagnosis", *IEEE Ultrasonic Symposium*, 2001, p1303-1306
3. D-R Chena, R-F Changb, C-J Chenb, M-F Hob, S-J Kuoa, S-T Chena, S-J Hungc, W-K Moond, "Classification of breast ultrasound images using fractal feature", Elseiver, *Journal of Clinical Imaging* Vol. 29, 2005, p 235-245
4. S Kim and S Yoon, "Bi-rads features-based computer-aided diagnosis of abnormalities in mammographic images". In 6th International Special Topic Conference on ITAB,(2007).
5. A Oliver, J Freixenet, R Marti, J Pont, E Prez, E-R-E. Denton and R Zwigelaar, "A Novel Breast Tissue Density Classification Methodology", *IEEE Transactions On Information Technology In Biomedicine*, Vol. 12, No. 1, January 2008, p55-65.
6. American College of Radiology "BI-RADS (Breast Imaging Reporting and Data System)" French Edition realized by SFR (Societe Francaise de Radiologie), Third Edition, 2003.
7. Alberta Program for the Early Detection of Breast Cancer. Alberta Cancer Board, 2001.
8. H Rangayyan, R., and J Desautels, "Content-based retrieval and analysis of mammographic masses". In *Journal of Electronic Imaging*.(2005).
9. The mammographic image analysis society digital mammogram database. In <http://www.wiau.man.ac.uk/services/MIAS/MIASweb.html>.

10. S Lam, Y., and Y Hong, "Blood vessel extraction based on mumford shah model and skeletonization". In Proceedings of the Fifth International Conference on Machine Learning and Cybernetics.(2006) Press.
11. B Jahne, "Digital image processing : concepts, algorithms, and scientific applications" (1993). In Springer-Verlag.
12. L Wei, Y Yang, R M. Nishikawa, and Yu Jiang "A Study on Several Machine-Learning Methods for Classification of Malignant and Benign Clustered Microcalcifications", IEEE Transactions On Medical Imaging, Vol. 24, NO. 3, March 2005, p371-380
13. K Djemal, W Puech and B Rossetto. Active Contours Propagation in a Medical Images Sequence With a Local Estimation, European Signal Processing Conference. EUSIPCO'02, Volume 1, pp: 41-44, September 2002, Toulouse, France.
14. I Cheikhrouhou, K Djemal, D Sellami, N Derbel and H Maaref "New mass description in mammographies". 1st International Workshops on Image Processing Theory, Tools & Applications, IPTA'08, Sousse, Tunisia, 24-26 November 2008.
15. I Cheikhrouhou, K Djemal, D Sellami Masmoudi, N Derbel and H Maaref. Abnormalities description for breast cancer recognition. Intenational Conference on E-Medical Systems, Morroco, 2007, p198-205.
16. K Djemal, W Puech and B Rossetto. Automatic Active Contours Propagation in a Sequence of Medical Images. International Journal of Images and Graphics. vol.6 , n. 2, pp :267-292 , 2006.
17. NR Mudigonda, RM Rangayyan, JEL Desautels: "Gradient and texture analysis for the classification of mammographic masses". IEEE Trans Med Imag 2000, p1032-1043.
18. K Djemal, F Bouchara and B Rossetto. Image Modeling and Regionbased Active Contours Segmentation. Int. Conf. Vision, Modeling and Visualization VMV'02, ISBN:3-89838-034-3, pp: 363-370, Novembre 2002, Erlangen, Germany.
19. R-M. Rangayyan and T-M. Nguyen "Fractal Analysis of Contours of Breast Masses in Mammograms", Journal of Digital Imaging, Vol 20, No 3, 2007, p223-237.
20. Q Guo, V Ruiz, J Shao, F Guo "A novel approach to mass abnormality detection in mammographic images", In Proceedings of the IASTED International Conference on Biomedical Engineering, Innsbruck, Austria, 2005, p180-185.
21. K Djemal. Speckle reduction in ultrasound images by minimization of total Variation. IEEE International Conference on Image Processing (ICIP), Volume 3, ISBN: 0-7803-9134-9, pp: 357-360, September 2005, Genova, Italya.
22. K Djemal, W Puech and B Rossetto. Geometric Active Contour Model Using Level Set Methods For Objects Tracking In Images Sequence. International Conference on Sciences of Electronics, Technology of Information and Telecommunication, SETIT'04, Mars 2004, Sousse, Tunisia.

